ChemComm

Cite this: *Chem. Commun.*, 2011, **47**, 6302–6304

www.rsc.org/chemcomm

COMMUNICATION

Improvement of (bipy)Pt(XR)$_2$ (X = O, S) type photosensitizers by covalent dye attachment†

Florian Pevny,[ab] Manfred Zabel,[a] Rainer F. Winter,*[ab] Andreas F. Rausch,[c] Hartmut Yersin,[c] Felix Tuczek[d] and Stanislav Záliš[e]

Received 15th October 2010, Accepted 4th April 2011
DOI: 10.1039/c0cc04443a

Irradiation into the dye-based absorption band of complexes (^{t}Bu$_2$bipy)Pt(SR)$_2$ and (^{t}Bu$_2$bipy)Pt(OR)$_2$ where R denotes a coumarine-based thiolate and alkoxolate substituent populates the same excited triplet state as is obtained by excitation into the much weaker (RX)$_2$Pt→^{t}Bu$_2$bipy (X = O, S) charge-transfer band. This paves the way toward more efficient photosensitizers.

Platinum diimine bis(alkynyl), bis(thiolate) or bis(alkoxolate) complexes (diimine)Pt(XR)$_2$ (XR = C≡CR, OR, SR) constitute a prominent class of photosensitizers with numerous applications in the fields of photocatalysis and light to (chemical) energy conversion;[1,2] *e.g.*, photocatalysed hydrogen production.[3,4] The photoreactive state is usually accessed by excitation into the (RX)$_2$Pt→diimine charge-transfer (CT) band with the strongly mixed metal alkynyl/thiolate/alkoxolate HOMO as the donor and a diimine based π* orbital as the acceptor orbital.[1,3,5,6] The charge-separated state thus generated may be reactive by itself or can be quenched by a sacrificial electron donor to yield the strongly reducing (diimine)Pt(XR)$_2^{\bullet-}$ as the reactive species.[3] Despite their tremendous success (diimine)-Pt(XR)$_2$-type photosensitizers usually suffer from the rather moderate absorption coefficient of the (RX)$_2$Pt→diimine CT band and from the limited spectroscopic window as defined by the envelope of the CT band that can be utilized to generate the photoreactive state. When considering the significant contributions of S or O atoms to the HOMO of diimine bis(thiolate) or -(alkoxolate) platinum complexes,[1,3,5,6] it occurred to us, that their incorporation into the extended π-system of an organic dye might serve to funnel the energy of a higher lying dye-based excited state into the lower lying ^{3}(RX)$_2$Pt→diimine CT state as it has already been demonstrated for coumarine-[Ru(terpy)$_2$]$^{2+}$-type dyads.[7] As a test of our hypothesis we prepared and investigated complexes **1–3** (see Chart 1) where the chalcogen donor atoms X are part of coumarine dyes. Coumarine dyes are particularly well suited for potential applications in photochemical hydrogen production owing to their stability in protic environments.

Complexes **1–3** were synthesized from (^{t}Bu$_2$bipy)PtCl$_2$ by simple salt metathesis with the respective hydroxylato or thiolato substituted coumarine.† In the solid state, complexes **1** and **2** possess the expected square planar platinum coordination with the Pt–N (2.051(5), 2.052(5)) and Pt–S (2.291(1), 2.293(1) Å, **1**) or Pt–N (range 1.992(7) to 2.012(6)) and Pt–O (range 2.009(6) to 2.026(8) Å for the three independent molecules of **2**) bond lengths in the usual range.‡ Both coumarine substituents are rotated out of the PtN$_2$S$_2$ or PtN$_2$O$_2$ planes by 67.1 or 83.7° (**1**) or 46.9 to 77.3° (**2**) (Fig. 1, Fig. S1, ESI†).

Absorption spectra of **1** and **2** in CH$_2$Cl$_2$ feature moderately intense ($\varepsilon \approx 3000$ M^{-1} cm^{-1}) asymmetric bands with maxima at 470 and 410 nm with a moderate negative solvatochromism and much more intense ($\varepsilon \approx 38\,000$ M^{-1} cm^{-1}) absorptions at 390 and 360 nm, respectively, as well as bands in the 320–300 nm range. All higher-energy bands display much lesser positional dependence on solvent polarity (Fig. S2–S4, ESI†). Literature precedence[1,3,5,6] suggests an assignment of the low-energy absorptions as (RX)$_2$Pt→^{t}Bu$_2$bipy$_1$* CT transition(s) with two or more underlying subbands. The intense band at higher

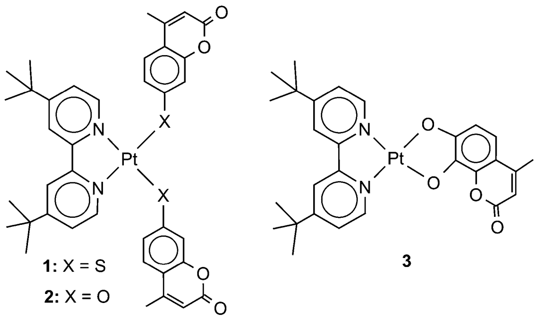

Chart 1 Complexes **1–3**.

---

[a] *Institut für Anorganische Chemie, Universität Regensburg, Universitätsstraße 31, D-93040 Regensburg, Germany*
[b] *Fachbereich Chemie, Universität Konstanz, Universitätsstraße 10, 78457 Konstanz, Germany. E-mail: rainer.winter@uni-konstanz.de; Fax: +49 7531 883136; Tel: +49 7531 885355*
[c] *Institut für Physikalische Chemie, Universität Regensburg, Universitätsstraße 31, D-93040 Regensburg, Germany*
[d] *Institut für Anorganische Chemie, Christian-Albrechts-Universität zu Kiel, Olshausenstraße 40, 24089 Kiel, Germany*
[e] *J. Heyrovský Institute of Physical Chemistry v.v.i., Academy of Sciences of the Czech Republic, Dolješkova 3, 182 23 Prague 8, Czech Republic*

† Electronic supplementary information (ESI) available: Synthetic procedures and characterization data; tables including structural data of complexes **1** and **2**; figures depicting the electronic spectra in various solvents, Raman spectra upon excitation at various wavelengths, representative voltammograms and representative results of spectro-electrochemical and quantum chemical studies. See DOI: 10.1039/c0cc04443a

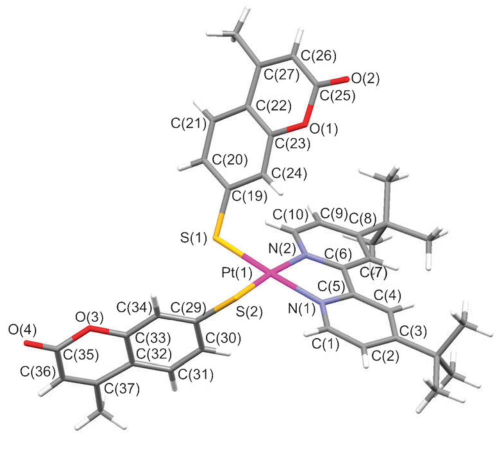

Fig. 1 Structure of complex **1** in the crystal.

energy is also composed of two or more underlying individual transitions and is more intense and significantly red shifted with respect to similar phenolate[6] or thiophenolate[6,8–10] bipyridine platinum complexes or the $\pi \rightarrow \pi^*$ bands of the corresponding free coumarine dyes. The bands near 320 and 300 nm finally resemble the ^{t}Bu$_2$bipy ligand-based $\pi \rightarrow \pi^*$ transitions in (^{t}Bu$_2$bipy)PtCl$_2$ (Fig. 2).

Experimental evidence for an assignment of the low energy bands as $(RX)_2Pt \rightarrow {}^tBu_2bipy_1{}^*$ CT comes from Resonance Raman spectroscopy of **1** with laser excitation at different wavelengths throughout the band envelope (see Fig. S5, S6, ESI†). All these spectra show bands attributable to vibrational modes of the ^{t}Bu$_2$bipy (1611, 1545, 1490, 1318, 1286, 1164, 1037, 770, 685 cm^{-1}) and the thiocoumarine ligands (1710, 1590, 1530, 1364, 1088, 720, 574, 520, 485, 382 cm^{-1}) as well as bands that probably originate from the Pt–S and Pt–N stretches (407, 400–300 cm^{-1}).[9–12] Merging the two phenolate oxygen atoms of **2** into the single catecholate ligand of **3** has the known effect of intensifying the low energy band ($\varepsilon \approx 6700$ M^{-1} cm^{-1}) and shifting it to lower energy ($\lambda_{max} = 520$ nm).[6] In accord with a coumarine based parentage, the intensity of the higher energy band at *ca.* 390 nm drops to $\varepsilon \approx 15\,000$ M^{-1} cm^{-1}, about half of that in complexes **1** or **2** (Fig. S4, ESI†). This is in accord with the presence of just one such π-chromophore in **3** as opposed to two in **1** and **2**.

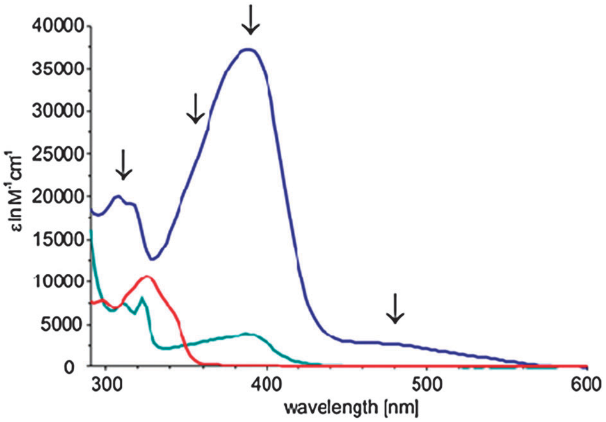

Fig. 2 Comparison of the UV/Vis spectra of (^{t}Bu$_2$bipy)PtCl$_2$ (green), the free thiocoumarine dye (red) and **1** (dark blue). The excitation wavelengths for the emission studies are indicated by arrows.

Electrochemistry provides a powerful probe of the energies and natures of the immediate frontier orbitals, in particular when combined with spectroscopy. Voltammetric measurements on **1** and **2** (CH$_2$Cl$_2$/0.1 M NBu$_4$PF$_6$) reveal an irreversible oxidation at +0.390 or +0.675 V (v = 0.20 V s^{-1}) and a reversible reduction at −1.840 V or −1.785 V, respectively (Fig. S7, ESI†). Alkoxylate *versus* thiolate substitution thus exerts a notable influence on the oxidation potential but hardly affects that of the reduction. For **3**, the oxidation was a chemically reversible process at $E_{1/2}$ = +0.170 V followed by a partially reversible second oxidation at +1.020 V, while the reduction occurred at −1.820 V. UV/Vis/NIR spectroscopic changes that accompany these redox processes indicate that the reductions are bipyridine-based as is indicated by the growth of the typical bipy$^{\bullet-}$ absorption bands near 370–410, 470, 505 and 810 nm for **1–3**$^{\bullet-}$ (Fig. S8, ESI†).[13] Based on the appearance of the typical semiquinonate absorption bands at 436, 451 nm as well as lower energy bands at 650 and 702 nm for **3**$^{\bullet+}$ (Fig. S9, ESI†), the reversible oxidation of **3** is assigned as the catecholate → semiquinonate type conversion,[6,14] while the second one most probably constitutes the semiquinonate/dioxolene process. All these findings conform to those on the body of similar bis(thiolate) or bis(alkoxolate) platinum bipyridine complexes and provide additional evidence for a (RX)$_2$Pt-based (**1**, **2**) or catecholate (**3**) based HOMO and a ^{t}Bu$_2$bipy based LUMO.

Like other dimine bis(phenolate) or -thiophenolate platinum systems, complexes **1–3** are luminescent when excited into their low-energy $(RX)_2Pt \rightarrow {}^tBu_2bipy$ absorption bands. Deaerated CH$_2$Cl$_2$ solutions of **1** and **2** exhibit very weak luminescence at ambient temperature in the red/near infrared spectral range with maxima at 790 nm (**1**) and 660 nm (**2**). These very weak emissions do not allow for a reliable determination of emission quantum yields and decay times. In frozen CH$_2$Cl$_2$ solutions (77 K), **1** and **2** are brightly emissive, while the phosphorescence of **3** is relatively weak. Maxima can be observed at 585 nm (**1**, Fig. 3), 530 nm (**2**, Fig. S10, ESI†) and 645 nm (**3**, Fig. S11, ESI†) with decay times (λ_{exc} = 375 nm) amounting to 2.1 μs and 7.4 μs for **1**, 4.0 μs for **2** and 1.3 μs for **3**. The relatively short decay times at 77 K, the broad and unresolved emission spectra and the very large rigidochromic blue shifts when going from fluid to frozen solutions are consistent with a $^3(RX)_2Pt \rightarrow {}^tBu_2bipy_1{}^*$ CT origin of the respective emissions, as is expected of this type

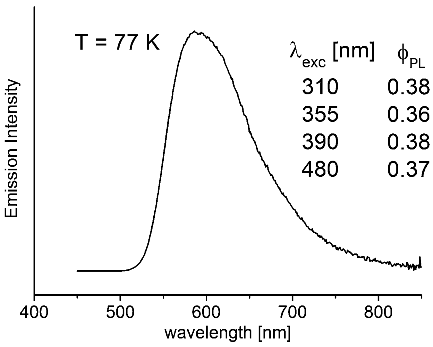

Fig. 3 Emission of complex **1** (CH$_2$Cl$_2$, 77 K) with quantum yields for different excitation wavelengths.

of complexes.[2,5,6,8] The emission quantum yields at 77 K after excitation into the low-energy (RX)$_2$Pt → ^{t}Bu$_2$bipy* absorption bands were determined to 0.37 (**1**), 0.57 (**2**) and ≈0.01 (**3**).

Most importantly, the same emission spectra are obtained when the compounds are excited at different higher energies (Fig. 2 and 3, S10, S11). Further, the emission quantum yields of **1** and **2** are independent of the excitation wavelength within the limits of the experimental error.§ This indicates complete energy transfer to the low lying CT triplet state even after excitation at 355 nm, corresponding to $\pi \rightarrow \pi^*$ transitions of the respective coumarine ligands. It is remarked that similar energy transfer from surface-bound, deprotonated thiocoumarine to CdSe quantum dots has recently been communicated.[15] In addition, excitation spectra of **1–3** recorded at their respective emission peaks retrace the absorption spectra with only slight rigidochromically induced peak shifts (Fig. S12, ESI†).

(TD) DFT quantum chemical calculations on complexes **1–3** were performed in order to investigate their electronic structures and the origins of the individual optical transitions. Calculated structures and spectral parameters (Table S5, ESI†) well reproduce the experimental data. An almost degenerate set of HOMO and HOMO−1 of **1** represents the π orbitals of the coumarine ligands with large contributions of the S atoms and about 10% contribution of Pt d_π orbitals. LUMO, LUMO + 3 and LUMO + 4 have bipy character whereas LUMO + 1 and LUMO + 2 are coumarine π* orbitals (Fig. 4). The low-energy CT band of **1** is assigned as Pt(SR) → bipy CT in agreement with our results from (spectro)-electrochemistry. The intense feature around 386 nm is composed of several transitions, the most intense one of which, f, is a $\pi \rightarrow \pi^*$ coumarine transition. The next optical band at higher energy is formed by LLCT and MLCT components.

Similar calculations on **3** show the strong participation of the coumarine-derived catecholato ligand to HOMO and HOMO−1. LUMO, LUMO + 1 and LUMO + 2 are all centred on the bipy ligand while LUMO + 3 is a coumarine π* orbital (Fig. S13, ESI†). The low-energy CT band of **3** is thus assigned as coumarine → bipy LLCT, while the optical band at 390 nm has LLCT and coumarine $\pi \rightarrow \pi^*$ components.

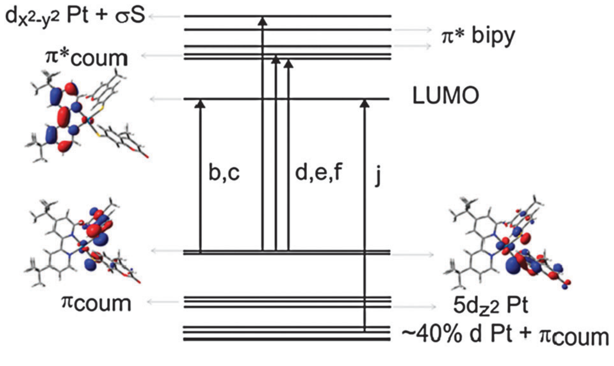

Fig. 4 Qualitative MO scheme for **1**. Arrows indicate the main contributions to the lowest allowed TD DFT calculated transitions.

While several complexes of oligopyridine ligands with appended π-chromophores have appeared in the literature there is only little precedence for the funnelling of the dye-based excitation energy into a long-lived photoreactive state. The latter principle is expected to lead to better sensitizers with significantly enhanced efficiencies and a much wider spectroscopic window available for their photoactivation. Work along these lines is under progress in our laboratories.

Financial support of this work by the Bundesministerium für Bildung und Forschung (BMBF) is gratefully acknowledged. We also wish to thank Ursula Cornelissen for conducting the Resonance Raman measurements. S.Z. thanks to the Ministry of Education of the Czech Republic (grant LD11086) for support.

Notes and references

‡ Crystal data for **1**: $C_{38}H_{38}N_2O_4PtS_2$, M = 845.92, monoclinic, $P21/c$, a = 15.3887(6) Å, b = 15.2435(6) Å, c = 15.5604(7) Å, β = 101.039(4)°, V = 4582.6(3) Å^3, Z = 4, T = 123 K, reflections: 12 795, 6134 independent (R_{int} = 0.0293), R_1 = 0.0568 for 5173 reflections $I > 2\sigma(I)$, wR_2 = 0.1488 (all data). Crystal data for **2**: $C_{38}H_{38}N_2O_6Pt$, M = 813.78, monoclinic, $P2/n$, a = 14.0527(3) Å, b = 15.6962(3) Å, c = 31.7532(8) Å, β = 99.169(2)°, V = 6914.4(3) Å^3, Z = 8, T = 123 K, reflections: 23 812, 10 719 independent (R_{int} = 0.0377), R_1 = 0.0530 for 7005 reflections $I > 2\sigma(I)$, wR_2 = 0.1462 (all data).

§ Due to the very low emission quantum yield of **3** even at 77 K, the errors in the quantum yields obtained at different excitation wavelengths are too high for a reliable comparison.

1 M. Hissler, J. E. McGarrah, W. B. Connick, D. K. Geiger, S. D. Cummings and R. Eisenberg, *Coord. Chem. Rev.*, 2000, **208**, 115–137.
2 E. A. M. Geary, L. J. Yellowlees, L. A. Jack, I. H. D. Oswald, S. Parsons, N. Hirata, J. R. Durrant and N. Robertson, *Inorg. Chem.*, 2005, **44**, 242–250.
3 S.-H. Hwang, C. N. Moorefield, F. R. Fronczek, O. Lukoyanova, L. Echegoyen and G. R. Newkome, *Chem. Commun.*, 2005, 713–715.
4 J. Zhang, P. Du, J. Schneider, P. Jarosz and R. Eisenberg, *J. Am. Chem. Soc.*, 2007, **129**, 7726–7727.
5 S. C. Cummings and R. Eisenberg, *J. Am. Chem. Soc.*, 1996, **118**, 1949–1960.
6 J. A. Weinstein, M. T. Tierney, E. S. Davies, K. Base, A. A. Robeiro and M. W. Grinstaff, *Inorg. Chem.*, 2006, **45**, 4544–4555.
7 K. Heinze and K. Hempel, *Chem.–Eur. J.*, 2009, **15**, 1347–1358.
8 J. A. Zuleta, J. M. Bevilacqua, D. M. Proserpio, P. D. Harvey and R. Eisenberg, *Inorg. Chem.*, 1992, **31**, 2396–2404.
9 J. A. Weinstein, N. N. Zheligovskaya, M. Y. Mel'nikov and F. Hartl, *J. Chem. Soc., Dalton Trans.*, 1998, 2459–2466.
10 J. A. Weinstein, A. Blake, E. S. Davies, A. L. Davis, M. W. George, D. C. Grills, I. V. Lileev, A. M. Maksimov, P. Matousek, M. Y. Mel'nikov, A. W. Parker, V. E. Platonov, M. Towrie, C. Wilson and N. N. Zheligovskaya, *Inorg. Chem.*, 2003, **42**, 7077–7085.
11 O. Poizat and C. Sourisseau, *J. Phys. Chem.*, 1984, **88**, 3007–3014.
12 F. Hartl, T. L. Snoeck, D. J. Stufkens and A. B. P. Lever, *Inorg. Chem.*, 1995, **34**, 3887–3894.
13 J. Víchová, F. Hartl and A. Vlček Jr., *J. Am. Chem. Soc.*, 1992, **114**, 10903–10110.
14 B. Sarkar, R. Hübner, R. Pattacini and I. Hartenbach, *Dalton Trans.*, 2009, 4653–4655.
15 M. González-Béjar, M. Frenette, L. Jorge and K. C. Scaiano, *Chem. Commun.*, 2009, 3202–3204.